Available online at www.sciencedirect.com
ScienceDirect
European Journal of Pharmaceutics and Biopharmaceutics 65 (2007) 10–17
European Journal of Pharmaceutics and Biopharmaceutics
www.elsevier.com/locate/ejpb

Research paper

Probing insulin's secondary structure after entrapment into alginate/chitosan nanoparticles

B. Sarmento [a,b,*], D.C. Ferreira [a], L. Jorgensen [b], M. van de Weert [b]

[a] Department of Pharmaceutical Technology, Faculty of Pharmacy of the University of Porto, Porto, Portugal
[b] Department of Pharmaceutics and Analytical Chemistry, The Danish University of Pharmaceutical Sciences, Copenhagen, Denmark

Received 10 February 2006; accepted in revised form 18 September 2006
Available online 24 September 2006

Abstract

The aim of the present study was to probe the structural integrity of insulin after being entrapped into chitosan/alginate nanoparticles produced by ionotropic polyelectrolyte pre-gelation. By manipulating the alginate:chitosan mass ratio and the pH during nanoparticle production, desired nanoparticles with a mean size of 850 (±88) nm and insulin association efficiency of 81 (±2)% were obtained. Insulin secondary structure was assessed by Fourier transform infrared (FTIR) and circular dichroism (CD) after entrapment into nanoparticles and after release from the particles under gastrointestinal simulated conditions. FTIR second-derivative spectra and area-overlap compared to an insulin standard confirmed that no significant conformational changes of insulin occurred in terms of α-helix and β-sheet content. Far-UV-CD spectra corroborated the preservation of insulin structure during the nanoparticle production procedure. The presented nanoparticulate system is a promising carrier for insulin oral delivery since it preserves insulin structure and therefore also, potentially, its bioactivity.

Keywords: Alginate; Chitosan; Circular dichroism; FTIR; Insulin; Nanoparticles; Secondary structure

1. Introduction

Many attempts to improve the gastrointestinal uptake of poorly absorbable drugs like insulin have been carried out [1,2]. A potential advantage of oral insulin delivery would be a hepatic versus systemic insulin ratio that more closely resembles that of the natural state compared to subcutaneous injections. Moreover, oral delivery may circumvent the reduced patient compliance associated to parenteral delivery.

Several natural [3,4] and synthetic [5–7] polymeric nanoparticulate systems are used for insulin entrapment. They can protect the labile molecule from degradation in the gastrointestinal tract and promote transport into the systemic circulation [4,6]. The latter is due to a prolonged adhesive contact with the absorptive gastrointestinal cells, and when the polymer matrix is in the nanometer size range, the particles may be taken up by the Peyer's patches [8]. Moreover, alginate ionotropic pre-gelation has been shown previously to be able to produce nanoparticles containing insulin [9].

Although nanoencapsulation shows promise for oral protein delivery, little attention has been paid to the effect of nanoencapsulation methodology on the protein structure. Different types of forces are responsible for insulin and general protein physicochemical stability, such as hydrophobic and electrostatic interactions, covalent bonding, hydrogen bonding and van der Waals forces. The complex interaction between these forces places hydrophobic residues in the interior of the protein while directing hydrophilic residues to the outside of the protein, where they interact with the aqueous solvent. Manipulation conditions of proteins can lead to conformational changes, thus exposing hydrophobic areas, resulting in reduced solubility and an increased tendency to aggregation [10]. Also,

* Corresponding author. Department of Pharmaceutical Technology, Faculty of Pharmacy of the University of Porto, Rua Aníbal Cunha 164, 4050-030 Porto, Portugal. Tel.: +351 222078900; fax: +351 222003977.
E-mail address: bruno.sarmento@ff.up.pt (B. Sarmento).

0939-6411/$ - see front matter © 2006 Elsevier B.V. All rights reserved.
doi:10.1016/j.ejpb.2006.09.005

physical forces related to various protein processes, such as stirring, pumping, filtration, chromatography and centrifugation, can expose proteins to air/liquid and liquid/solid interfaces resulting in similar undesired effects and loss of structural integrity.

The aim of this study was to determine the structural integrity of insulin upon entrapment in alginate/chitosan nanoparticles produced by ionotropic polyelectrolyte pre-gelation. Because of their large application on the protein physical stability analysis [10–15], Fourier transform infrared (FTIR) and circular dichroism (CD) spectroscopy have been used in this study to examine the insulin structure and interactions between insulin and polymeric matrices after entrapment.

2. Materials and methods

2.1. Materials

Low-G ($F_G = 0.39$) low viscosity sodium alginate, chitosan low MW (≈50 kDa), and calcium chloride were purchased from Sigma (Sintra, Portugal). Polyanion stock solutions were prepared in deionized water (Milli-Q®) overnight under magnetic stirring and chitosan samples were dissolved in 1% acetic acid solution in deionized water followed by filtering using a Millipore #2 paper filter and stored at 4 °C. Human crystalline zinc-insulin was a gift from Lilly Portugal.

2.2. Particle preparation

Alginate/chitosan particles were prepared in a two-step procedure based on the ionotropic pre-gelation of polyanion with calcium chloride followed by polycationic cross-linking through a adapted protocol initially described by Rajaonarivony et al. [16], but modified according to ideal pre-gelation stoichiometric ratio and time of drug association [17]. 7.5 ml of 18 mM calcium chloride solution was added dropwise for 60 min under gentle stirring (800 rpm) into a beaker containing 117.5 ml of a 0.063% alginate solution to provide an alginate pre-gel. Then, 25 ml of different concentration (0.05–0.09%) chitosan solution was added dropwise into the pre-gel over 90 min. The pH of alginate and chitosan solutions was initially set to 4.9 and 4.6, respectively. A colloidal dispersion at pH 4.7 formed upon polycationic chitosan addition, visible as the Tyndall effect. Nanoparticles were stirred for 30 min to improve curing and subsequently collected by centrifugation (20,000*g*/45 min) at 4 °C. For insulin-loaded nanoparticles, 7 mg of insulin (equivalent to 200 IU) was mixed with the alginate solution before calcium chloride addition.

2.3. Nanoparticle size analysis

The average of 30 size readings was assessed by photon correlation spectroscopy (PCS) using a Malvern Zetasizer and Particle Analyzer 5000 (Malvern Instruments, UK). Five milliliters of sample was gently shaken, placed into the analyzer chamber and readings were performed at 25 °C with a detected angle of 90°. Results are given in *z*-average (±SD).

2.4. FTIR analysis

IR-spectra were measured using a Bomem IR-spectrometer (Bomem, Canada). The hydrated samples were placed in a cell with CaF_2 crystal windows and a 6 μm spacer. For solid samples, aliquots corresponding to 2 mg of insulin were gently mixed with 300 mg of micronized KBr powder and compressed into discs at a force of 10 kN for 2 min using a manual tablet press (Perkin-Elmer, Norwalk, USA). For each spectrum a 256-scan interferogram was collected with a 4 cm^{-1} resolution in the mid-IR region at room temperature. Insulin spectra were obtained according to a double subtraction procedure [18] and insulin-free systems and water vapor spectra were collected under identical conditions for blank subtraction. The second-derivative spectra were obtained with a seven-point Savitsky–Golay derivative function and the baseline was corrected using a 3–4 point adjustment. In addition, the spectra were area-normalized in the amide I region from 1710 to 1590 cm^{-1} using the Bgrams software (Galactic Industries, Salem, NH) and area-overlap compared to an insulin aqueous standard solution of 10 mg/ml, in an appropriated buffer (Origin® software). All samples were run in duplicate and the data presented are the average of the two measurements.

2.5. Circular dichroism analysis

CD spectra were obtained at room temperature on an Olis DSM 10 Spectrophotometer (Georgia, USA), using an insulin concentration of 0.2 mg/ml. In the far-UV region CD spectra were recorded in a 0.01 cm cell from 250 to 190 nm, using a step size of 0.5 nm, a bandwidth of 1.5 nm, and an averaging time of 5 s, with the lamp housing purged with nitrogen to remove oxygen. For all spectra, an average of 5 scans was obtained. CD spectra of the appropriate reference were recorded and subtracted from the protein spectra. The molar ellipticity for insulin was calculated as the CD signal × MRW (115 Da, mean residual weight of each insulin residue) [insulin concentration (mg/ml) × cell path length (0.1 mm)]. Insulin concentration was determined by UV absorption at 276 nm using an extinction coefficient of 1.08 for 1.0 mg/ml [11].

2.6. Insulin association efficiency (AE) and loading capacity (LC)

The AE was determined indirectly after separation of nanoparticles from the aqueous medium containing non-associated insulin. The amount of insulin associated with the particles was calculated by the difference between the

total amount used to prepare the particles and the amount of insulin present in the aqueous phase after centrifugation.

$$\mathrm{AE} = \frac{\text{Total amount of insulin} - \text{Free insulin in supernatant}}{\text{Total amount of insulin}} \times 100$$

The difference between the total insulin amount initially used to prepare the particles and the amount of residual unassociated insulin after particle separation as a percent of total nanoparticle dry mass is referred to as LC. Dry mass was obtained by freeze-drying an aliquot of hydrated nanoparticle obtained after isolation.

$$\mathrm{LC} = \frac{\text{Total amount of insulin} - \text{Free insulin in supernatant}}{\text{Total dry weight of nanoparticles}} \times 100$$

Insulin was determined by HPLC [19]. Briefly, a Varian HPLC was equipped with an XTerra RP 18 column, 5 μm particle size, 4.6 mm internal diameter × 250 mm length (Waters®, USA) and a LiChrospher® 100 RP-18, 5 μm particle size guard column (Merck, Germany) and a mobile phase gradient composed of acetonitrile (ACN) and 0.1% trifluoroacetic acid (TFA) aqueous solution were used at a flow rate of 1 ml/min. Protein identification was made by UV detection at 214 nm. The gradient linearly changed from 30:70 (ACN: TFA) to 40:60 in 5 min running followed by 5 min isocratic 40:60 ratio. The method was validated and found to be linear in the range of 1–100 μg/ml ($R^2 = 0.9996$). The total peak area was used to quantify the insulin.

2.7. Evaluation of insulin in vitro release from nanoparticles

Nanoparticles were placed either into test tubes with simulated gastric fluid (SGF) containing 20 ml of HCl pH 1.2 USP XXVI buffer (100 rpm) and simulated intestinal fluid (SIF) containing 20 ml of phosphate, pH 6.8, USP XXVI buffer (100 rpm). At appropriate intervals aliquots were taken and replaced by fresh medium. The amount of insulin released from the nanoparticles was evaluated by HPLC.

3. Results and discussion

3.1. Nanoparticle characterization

The main purpose of this work was to elucidate the effect on the secondary structure of insulin after entrapment into alginate/chitosan nanoparticles by ionotropic pre-gelation. Prior to insulin structural assessment assays, nanoparticles were characterized with respect to their mean size, AE and LC. The results of characterization of different nanoparticles are shown in Table 1.

The mean particle size, AE and LC of the nanoparticles were affected by the initial ratio between the mass of alginate and chitosan used to prepare the nanoparticles. Decreasing the alginate:chitosan mass ratio from 6:1 to 3.3:1 led to an increase in AE and a decrease of the LC.

Table 1
Characterization of alginate/chitosan nanoparticles produced at different conditions in terms of mean nanoparticle size (±SD), insulin association efficiency (AE) and loading capacity (LC) as a function of alginate: chitosan mass ratio ($n = 3$)

Alginate: chitosan mass ratio	pH of production	Mean size (nm)	AE (%)	LC (%)
6:1	4.7	779 ± 100	69 ± 2	9.8 ± 0.7
3.3:1	4.7	1669 ± 210	91 ± 1	6.5 ± 0.2
4.3:1	4.2	1858 ± 174	83 ± 2	4.7 ± 0.2
4.3:1	4.7	850 ± 88	81 ± 1	9.9 ± 0.6
4.3:1	5.2	1062 ± 210	60 ± 3	8.5 ± 1.4

Also, the mean particle size increased with the decrease in alginate:chitosan mass ratio reaching the microsize range.

The effect of pH on nanoparticle formation was also examined. The pH range was chosen to achieve opposite charges of polyelectrolytes and ideal nanocomplex formation. At this pH range electrostatic interactions take place between polymers and proteins. The decrease of pH from 4.7 to 4.2 led to a slight increase of AE. However, when the pH of the aqueous solution was set to 4.2, the particles became much larger (>1 m) and the LC decreased. In this pH range alginate approaches its pK_a value (~3.5) and a small part of it starts to precipitate as alginic acid. The precipitated alginate can contribute to the increased mean particle size measured by photon correlation spectroscopy and to the decrease in LC because some of the recovered nanoparticle mass was composed merely of insoluble alginate. Consequently, insulin was partially bound ionically to insoluble alginic acid. Similar conclusions, to a lesser extent, can be drawn when the pH of nanoparticle formation was increased from 4.7 to 5.2, where chitosan precipitation may occur (p$K_a \sim 6$). Alginate/insulin interactions are the first to occur during the nanoparticle production process and alginate is present in higher concentration than chitosan, thus the AE is probably more dependent on opposing charges between alginate and insulin than between chitosan and insulin. At pH 4.2, insulin is mainly positively charged (pI 5.3) and thus interacts with the partially negative alginate, while at pH 5.2 there are less positive charges on the protein that can interact with the negative charges on the alginate. Consequently, the insulin AE is decreased at pH 5.2. Therefore, pH 4.7 where nanoparticles were formed and high insulin association efficiency was obtained was chosen in the subsequent experiments.

To study the potential of these nanoparticles for oral insulin delivery, the cumulative release profile in both simulated gastric (SGF) and intestinal (SIF) conditions was determined. Fig. 1A displays the cumulative release profiles of insulin from alginate/chitosan nanoparticles with different alginate:chitosan mass ratio under SGF. It shows that insulin release from different nanoparticles occurred very rapidly during the first 5 min of the assay; afterwards it was considerably slowed down. Up to 50% insulin was released in a burst effect for all three formulations studied.

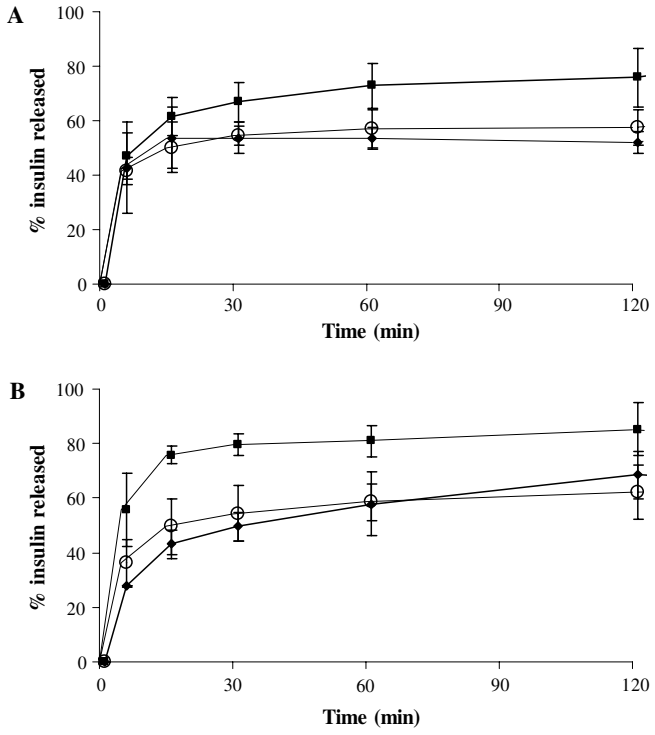

Fig. 1. Cumulative insulin release in SGF (A) and SIF (B) from insulin-loaded alginate/chitosan prepared at pH 4.7 produced with alginate–chitosan mass ratio of 6:1 (■), 4.3:1 (♦) and 3.3:1 (○) ($n = 3$, bars represent SD).

Probably, a significant amount of insulin was associated to the surface of the nanoparticles, because the alginate nuclei did not have the capacity to entrap all protein. However, the decrease in the amount of chitosan in the formulation led to a further increase in released insulin. After 120 min in SGF, nanoparticles with an alginate:chitosan mass ratio of 6:1 released 75.9% of insulin, 18% more than nanoparticles with an alginate:chitosan mass ratio of 4.3:1. These results seem to indicate a protective role of chitosan against insulin diffusion from the alginate matrix due to the formation of an alginate/chitosan complex film on the surface of the nanoparticles. The effect of the alginate/chitosan interaction on the sustaining of protein release has previously been observed by others [20,21]. However, the significant release over a 2-h period indicates that further optimization of the system is still required, in order to increase the amount of insulin released in the intestine rather than in the stomach.

The cumulative release profile of insulin from the same formulations in SIF is shown in Fig. 1B. All formulations resulted in a significant insulin burst release, more evident for the formulation containing an alginate:chitosan mass ratio of 6:1 and less pronounced for the alginate:chitosan mass ratio of 4.3:1. Also, for all formulations the release pattern was similar to those in the GSF, but with slightly higher cumulative amounts. Here, also, additional chitosan at an alginate:chitosan mass ratio of 3.3:1 did not yield a significantly different cumulative profile than the 4.3:1 ratio. After 120 min, the amount of insulin released from nanoparticles was around 10% higher than in GSF for all formulations. After 24 h of release study, almost 100% of entrapped insulin was released from nanoparticles (results not shown).

3.2. Structural analysis

The second-derivative FTIR spectrum of insulin in solution is presented in Fig. 2. Insulin is dominated by α-helix content (1654 cm^{-1}), but also β-sheet and β-turn minor components (1684 and 1632 cm^{-1}) are present [12,22]. The spectrum of insulin solution prepared at pH 4.7 was almost equal to that at pH 1.2, presenting an area-overlap of 0.98 indicating that the native conformation was practically unchanged in this pH range.

FTIR insulin spectra were also collected after insulin encapsulation. Fig. 2 represents spectra of insulin entrapped into nanoparticles (alginate:chitosan mass ratio 4.3:1) collected immediately after production and after one month of storage. The results indicate that the insulin structure was, in general, only slightly affected after association with the nanoparticles. The α-helix band became narrower after encapsulation, but visually it appears to keep the same area intensity. Ionic interactions that occur between opposite charges of the protein and the polymers could be responsible for small rearrangements of the protein structure and a simple subtraction of empty nanoparticles spectrum may not be complete because the protein also slightly affects the polymers through ionic interactions. However, the main peaks corresponding to β-sheet and especially α-helix remained almost unchanged, which indicates that the protein secondary structure was not significantly altered.

The area-overlap reflects the degree of overall structural changes of proteins upon incorporation. The area-overlap between insulin spectrum in acetate buffer, pH 4.7, and

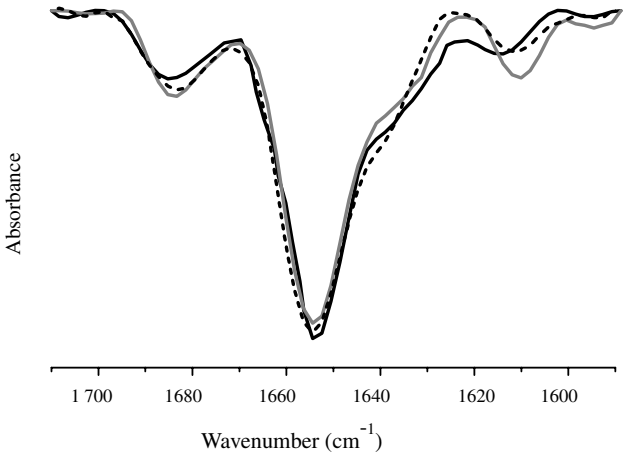

Fig. 2. Second-derivative FTIR spectrum of human insulin 10 mg/ml in 0.01 M HCl, pH 1.2 (——), entrapped into fresh alginate/chitosan nanoparticles (▪▪▪▪▪) and entrapped into stored alginate/chitosan nanoparticles (——) ($n = 2$).

insulin spectra entrapped into fresh and stored nanoparticles (one month) was found to be 0.95 (±0.01) and 0.94 (±0.02). The structural changes of insulin after one month entrapped into nanoparticles were very similar to insulin in nanoparticles without storage, which is a good indicator of formulation stability in terms of maintaining protein structure during the period of time studied (Table 2).

The influence of pH in the nanoparticle formation and the alginate:chitosan mass ratio on entrapped insulin structure was also determined and results are shown in Fig. 3. The pH during nanoparticle production appeared to be responsible for small differences between entrapped insulin structures. Variation of pH in the nanoparticle formation from 4.2 to 5.2 caused a variation in the area-overlap from 0.95 (±0.01) to 0.90 (±0.01) (Table 3) when compared to an insulin solution at pH 4.7. Two effects can explain this behaviour. Firstly, different degrees of insulin protonation in the pH range could lead to small differences in secondary structure. Secondly, due to the ionic nature of interaction between polymers and insulin, different pH values made insulin more or less vulnerable to deviations from the native structure, mainly on the surface of the insulin molecule. Nevertheless, nanoparticles produced at pH 4.7 appear to have little effect on insulin secondary structure, cf. Table 3.

Variation of alginate:chitosan mass ratio on nanoparticle production presented a less pronounced effect on change in insulin secondary structure, cf. Fig. 3B. Visually, no significant protection or destabilization of insulin was found in the mass ratio range studied, which is also supported by the area-overlap values (Table 3).

Subsequently, the structure of insulin was studied after release from nanoparticles in different pH environments. As control, free insulin in solution was placed under agitation under the same conditions as the nanoparticles, and after 2 h samples for FTIR were collected. The area-overlap of insulin solution after 2 h in contact with pH 1.2 buffer vs the standard insulin solution was 0.97 (±0.01) ($n = 2$). These results indicate the absence of any significant insulin fibrillation, although it has been shown that low pH accelerates fibrillation [23]. This discrepancy with results in the literature can possibly be explained by the time interval and speed of stirring chosen to simulate the passage of nanoparticles through gastric environment, conditions which were less severe than those used by Nielsen et al. Insulin fibrils are characterized by an increase in β-sheet bands and a simultaneous decrease in α-helix, but these changes were not observed in the present case.

More extensive changes were observed at pH 6.8 where the area-overlap of insulin after 2 h in contact with pH 6.8 buffer vs the standard insulin solution was 0.92 (±0.02)

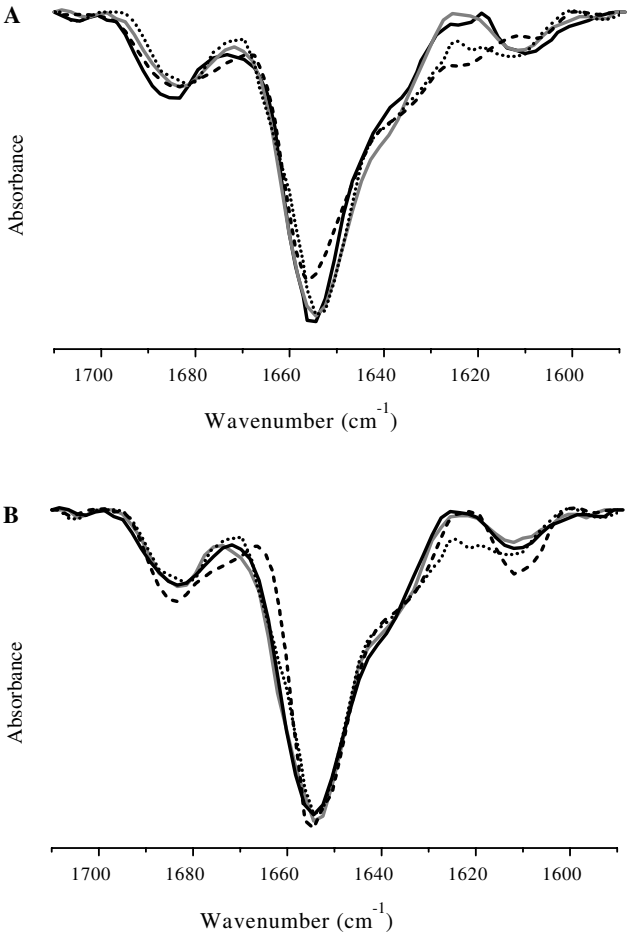

Fig. 3. (A) Second-derivative FTIR spectrum of human insulin in solution, 10 mg/ml, acetate buffer, pH 4.7 (▪▪▪▪▪) and entrapped into fresh nanoparticles produced with alginate:chitosan mass ratio of 4.3:1 prepared at pH 5.2 (——), 4.7 (——) and 4.2 (— — —). (B) Second-derivative FTIR spectrum of human insulin in solution at pH 4.7 (▪▪▪▪▪) and entrapped into fresh nanoparticles produced at pH 4.7 with alginate:chitosan mass ratio of 6.0:1 (——), 4.3:1 (——) and 3.3:1. (— — —) ($n = 2$).

Table 2
Area-overlap of baseline-corrected area normalized FTIR-spectra of freshly prepared insulin entrapped in alginate/chitosan nanoparticles and after storage compared with insulin in solutions at various pH ($n = 2$)

Insulin-loaded alginate/chitosan nanoparticle	Area-overlap pH 1.2[a]	Area-overlap pH 4.7[b]
Fresh	0.90 (±0.01)	0.95 (±0.01)
Stored	0.89 (±0.01)	0.94 (±0.02)

[a] vs 10 mg/ml insulin solution in 0.01 M HCl, pH 1.2.
[b] vs 10 mg/ml insulin solution in acetate buffer, pH 4.7.

Table 3
Area-overlap of baseline-corrected area normalized spectra of an insulin solution[a] and insulin entrapped in alginate/chitosan nanoparticles produced at different pH and alginate:chitosan mass ratio conditions ($n = 2$)

Alginate:chitosan mass ratio	pH of production	Area-overlap[a]
6.0:1	4.7	0.97 (±0.02)
3.3:1	4.7	0.93 (±0.02)
4.3:1	4.2	0.92 (±0.01)
4.3:1	4.7	0.95 (±0.01)
4.3:1	5.2	0.90 (±0.01)

[a] vs 10 mg/ml insulin solution in acetate buffer, pH 4.7.

($n = 2$) which could be attributed to a different protonation of insulin. Since its p*I* is around 5.3, at pH 6.8 insulin is negatively charged and with a different overall charge also a small alteration of secondary structure can be hypothesized. In fact, the FTIR spectrum of insulin in phosphate buffer 10 mM at pH 7.4, a pH value close to pH 6.8, presented a more apparent β-sheet band in the range of 1685–1695 cm^{-1} [22] than spectra obtained in both pH 1.2 and 4.7 buffers.

These observations are very useful when comparing FTIR insulin spectra after release from nanoparticle formulations in various pH solutions. Spectra are shown in Fig. 4 for nanoparticles with alginate:chitosan mass ratio of 4.3:1 prepared at pH 4.7. The FTIR spectra of insulin released from nanoparticles were comparable to the FTIR spectra of entrapped insulin but the band for α-helix increased in magnitude. The area-overlap was determined as 0.95 (±0.01) for entrapped insulin, 0.92 (±0.02) for insulin released at pH 1.2, and 0.94 (±0.01) for insulin released at pH 6.8. According to these values, structural changes observed after entrapment remained after insulin was released. However, more insulin was released from the nanoparticles at intestinal pH compared to gastric pH. After 120 min, a substantial fraction of insulin was still associated to nanoparticles (i.e., not released) and it is possible that this associated insulin contributed to the FTIR spectra. The area-overlap of insulin released at pH 6.8 is more consistent with free insulin, although possibly the polymer signal could not be completely subtracted using a blank formulation as in the gastric assay.

The insulin solutions were also analyzed using circular dichroism (CD) spectroscopy. The CD spectrum of 0.2 mg/ml insulin standard solution in 0.01 M HCl displays two minima at 209 and 222 nm, which is typical of predominant α-helix structure proteins. It is in close agreement with the spectra obtained by other authors [15,24]. Also, the CD spectra of different pH standard solutions, concretely 4.7 and 6.8, were found to be coincident with the ones collected at pH 1.2, which indicated that in these conditions pH variation was not responsible for significant changes in α-helix/β-sheet structure. Similar conclusions were drawn from the FTIR spectra.

After entrapment in alginate/chitosan nanoparticles, only minor differences were observed in the insulin spectrum (Fig. 5A). No substantial alterations were noted in the two α-helix minima but a slight shift around 205 nm could be observed. Probably, this shift occurs due to interference from the polymers on the nanoparticles, which cannot be eliminated by subtraction of insulin-free formulation. Similar issues were identified in the FTIR spectral analysis but the rise in signal for the CD spectra may well be due to scattering, while in the FTIR spectrum there could be a change in the absorbance of the nanoparticles upon insulin adsorption.

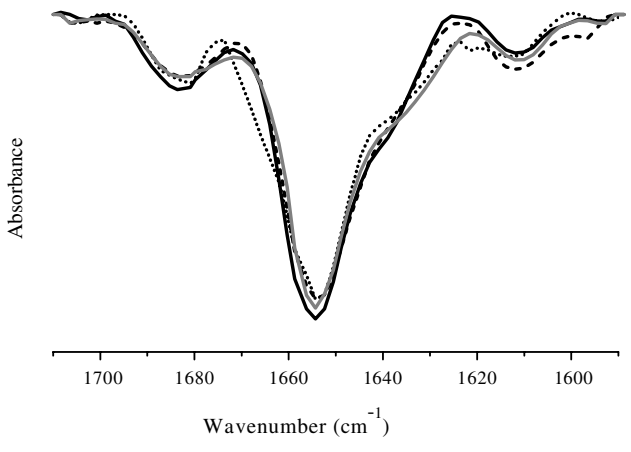

Fig. 4. Second-derivative FTIR spectrum of human insulin in solution, 10 mg/ml acetate buffer, pH 4.7 (▪▪▪▪▪), insulin entrapped into fresh alginate/chitosan nanoparticles (——), insulin released into USPXXVI HCl, pH 1.2, buffer from alginate/chitosan nanoparticles (——) and insulin released into USPXXVI Phosphate, pH 6.8, buffer from alginate/chitosan nanoparticles (— — —) prepared with alginate:chitosan mass ratio of 4.3:1 and prepared at pH 4.7 ($n = 2$).

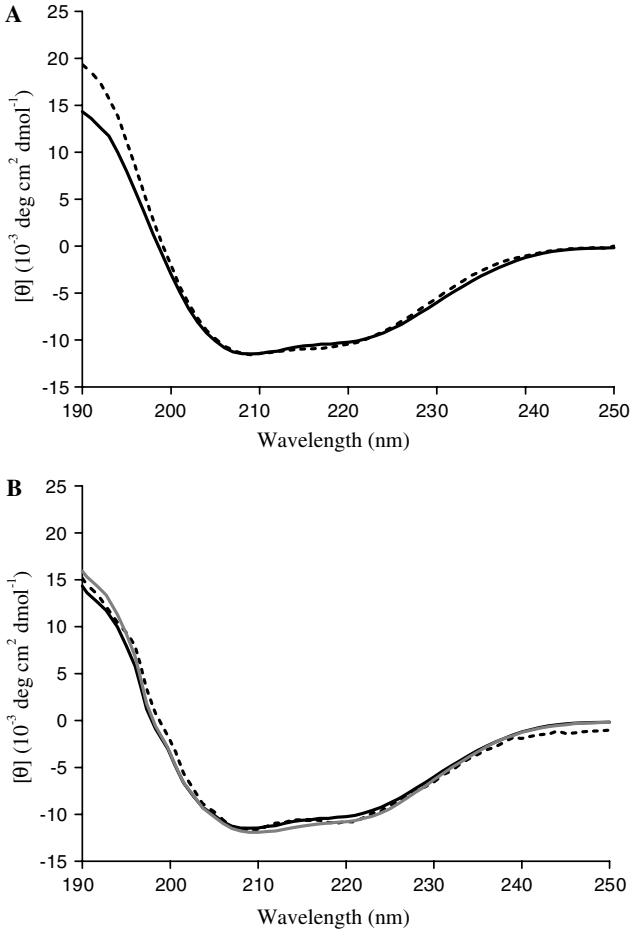

Fig. 5. (A) Far-UV CD spectrum of human insulin in 0.01 M HCl solution (——) and entrapped in alginate/chitosan nanoparticles prepared with alginate:chitosan mass ratio of 4.3:1 at pH 4.7 (▪▪▪▪▪). (B) Far-UV CD spectrum of human insulin in solution (——), insulin released into pH 1.2 buffer from alginate/chitosan nanoparticles (▪▪▪▪▪) and insulin released into pH 6.8 buffer from alginate/chitosan nanoparticles (——) prepared with alginate:chitosan mass ratio of 4.3:1 prepared at pH 4.7.

Insulin spectra after release in both simulated gastric and intestinal environments were collected to investigate potential changes in insulin structure. Fig. 5B shows the results of these studies. Insulin released from alginate/chitosan nanoparticles at pH 1.2 produced only minor differences compared with entrapped insulin. However, free insulin after 2 h agitation at pH 1.2 did not show an altered structure compared to standard insulin. Perhaps some influence from the nanoparticle components could explain this small difference, because such a difference was not observed when insulin was released from the same formulation at pH 6.8. At low pH the degree of interaction between insulin and alginate is higher and, therefore, ionic interactions are more favorable. Thus, some spectral changes could come from the ionic interaction.

It was observed by FTIR assessments that the pH of nanoparticle formation in the range of 4.2–5.2 and an alginate:chitosan mass ratio between 6:1 and 3.3:1 were only minor parameters of influence to changes in insulin secondary structure. To confirm this trend, the same structure of insulin after being released from nanoparticles produced with different alginate:chitosan mass ratio and different pH values of preparation were analyzed by far-UV-CD experiments. For all formulations, CD spectra were very similar to the insulin standard solution, suggesting minor, if any, changes of insulin secondary structure after being release from nanoparticles (data not shown). Thus, these systems seem to be stable to carry insulin and release it, while preserving structure and thus, potentially, also maintaining insulin activity.

Brange et al. observed that the rate of insulin fibrillation was higher in acid environments than at neutral pH, and increases with an increase in insulin concentration and an increase of temperature [25]. The low concentration of insulin and performing the preparation at room temperature in the present method to produce the insulin-loaded nanoparticles contributes to a low fibrillation rate [11]. Consequently, it is reasonable to assume that insulin did not fibrillate during nanoparticles production, which takes 120 min, and during the storage. Neither the proposed method for nanoparticle formation nor the natural polysaccharides used as nanoparticulate carrier matrix acted as stress factors for insulin instability, as often reported for other polymers and/or methods [14].

The fibrillation process of insulin could be one of the obstacles to assure structural preservation of insulin after entrapment. However, both FTIR and CD analysis did not indicate any fibril formation. Furthermore, extending the release time of insulin from nanoparticles to more than two hours, almost 100% of entrapped insulin was released from nanoparticles, according to HPLC assessments (data not shown). As insulin fibrils are insoluble in most aqueous media [25], 100% of insulin present in chromatographs also indicate an absence of fibrils both in free insulin solution as well as in insulin released from nanoparticles.

4. Conclusions

In this work, the effect of insulin entrapment into alginate/chitosan micro- and nanoparticles on its secondary structure has been examined. Formation of alginate/chitosan micro- or nanoparticles was dependent on alginate:chitosan mass ratio and pH of production. Insulin-loaded nanoparticles were successfully produced at pH 4.7 and with alginate:chitosan mass ratio of 4.3:1 and with a high insulin association efficiency. It was shown by FTIR and CD assessments that insulin preserved its intrinsic conformation after the entrapment process and following release in both gastric and intestinal simulated conditions. However, a further optimization of the release characteristics is required to reduce the release in the low-pH gastric environment, while maintaining a high release in the intestinal environment.

In conclusion, polyelectrolyte ionotropic pre-gelation appears to be a promising approach to produce nanoparticles containing insulin, as well as potentially other therapeutic polypeptides for oral delivery. However, the profile of protein released needs to be further optimized because burst release is not desired. Present studies are examining the control of release properties and insulin oral bioavailability after encapsulation in alginate/chitosan nanoparticles.

Acknowledgements

This work was supported by Fundação para a Ciência e Tecnologia, Portugal. The authors wish to thank Lilly Portugal for supply of insulin. Novo Nordisk A/S is acknowledged for funding of the Bomem FTIR spectrometer.

References

[1] F. Cui, K. Shi, L. Zhang, A. Tao, Y. Kawashima, Biodegradable nanoparticles loaded with insulin–phospholipid complex for oral delivery: preparation, in vitro characterization and in vivo evaluation, J. Control. Release 114 (2006) 242–250.
[2] Z. Ma, T.M. Lim, L.-Y. Lim, Pharmacological activity of peroral chitosan-insulin nanoparticles in diabetic rats, Int. J. Pharm. 293 (2005) 271–280.
[3] R. Fernandez-Urrusuno, P. Calvo, C. Remunan-Lopez, J.L. Vila-Jato, M.J. Alonso, Enhancement of nasal absorption of insulin using chitosan nanoparticles, Pharm. Res. 16 (1999) 1576–1581.
[4] Y. Pan, Y.J. Li, H.Y. Zhao, J.M. Zheng, H. Xu, G. Wei, J.S. Hao, F.D. Cui, Bioadhesive polysaccharide in protein delivery system: chitosan nanoparticles improve the intestinal absorption of insulin in vivo, Int. J. Pharm. 249 (2002) 139–147.
[5] C. Damge, H. Vrancks, P. Balschmidt, P. Couvreur, Poly(alkyl cyanoacrylate) nanospheres for oral administration of insulin, J. Pharm. Sci. 86 (1997) 1407–1500.
[6] G.P. Carino, J.S. Jacob, E. Mathiowitz, Nanosphere based oral insulin delivery, J. Control. Release 65 (2000) 261–269.
[7] X.Y. Ma, G.M. Pan, Z. Lu, J.S. Hu, J.Z. Bei, J.H. Jia, S.G. Wang, Preliminary study of oral polylactide microcapsulated insulin in vitro and in vivo, Diabetes Obes. Metab. 2 (2000) 243–250.
[8] T. Jung, W. Kamm, A. Breitenbach, E. Kaiserling, J.X. Xiao, T. Kissel, Biodegradable nanoparticles for oral delivery of peptides: is there a role for polymers to affect mucosal uptake? Eur. J. Pharm. Biopharm. 50 (2000) 147–160.

[9] B. Sarmento, S. Martins, A. Ribeiro, F. Veiga, R. Neufeld, D. Ferreira, Development and comparison of different nanoparticulate polyelectrolyte complexes as insulin carriers, Int. J. Pept. Res. Ther. 12 (2006) 131–138.
[10] O.C. Tatford, P.T. Gomme, J. Bertolini, Analytical techniques for the evaluation of liquid protein therapeutics, Biotechnol. Appl. Biochem. 40 (2004) 67–81.
[11] L. Nielsen, S. Frokjaer, J. Brange, V.N. Uversky, A.L. Fink, Probing the mechanism of insulin fibril formation with insulin mutants, Biochemistry 40 (2001) 8397–8409.
[12] L. Nielsen, S. Frokjaer, J. Carpenter, J. Brange, Studies of the structure of insulin fibrils by fourier transform infrared (FTIR) spectroscopy and electron microscopy, J. Pharm. Sci. 90 (2001) 29–37.
[13] M. van de Weert, M.B. Andersen, S. Frokjaer, Complex coacervation of lysozyme and heparin: complex characterization and protein stability, Pharm. Res. 21 (2004) 2354–2359.
[14] M. van de Weert, W.E. Hennink, W. Jiskoot, Protein instability in poly(lactic-co-glycolic acid) microparticles, Pharm. Res. 17 (2000) 1159–1167.
[15] W. Tiyaboonchai, J. Woiszwillo, R.C. Sims, C.R. Middaugh, Insulin containing polyethylenimine–dextran sulfate nanoparticles, Int. J. Pharm. 255 (2003) 139–151.
[16] M. Rajaonarivony, C. Vauthier, G. Couarraze, F. Puisieux, P. Couvreur, Development of a new drug carrier made from alginate, J. Pharm. Sci. 82 (1993) 912–917.
[17] B. Sarmento, A. Ribeiro, F. Veiga, R. Neufeld, D. Ferreira, Insulin-loaded alginate/chitosan nanoparticles produced by ionotropic pre-gelation, Rev. Port. Farm. LII (2005) 139–140.
[18] A. Dong, P. Huang, W.S. Caughey, Protein secondary structures in water from second-derivative amide I infrared spectra, Biochemistry 29 (1990) 3303–3308.
[19] B. Sarmento, A. Ribeiro, F. Veiga, D. Ferreira, Development and validation of a rapid reversed-phase HPLC method for the determination of insulin from nanoparticulate systems, Biomed. Chromatogr. 20 (2006) 898–903.
[20] C.-H. Zheng, J.-Q. Gao, Y.-P. Zhang, W.-Q. Liang, A protein delivery system: biodegradable alginate–chitosan-poly(lactic-co-glycolic acid) composite microspheres, Biochem. Biophys. Res. Commun. 323 (2004) 1321–1327.
[21] A.J. Ribeiro, C. Silva, D. Ferreira, F. Veiga, Chitosan-reinforced alginate microspheres obtained through the emulsification/internal gelation technique, Eur. J. Pharm. Sci. 25 (2005) 31–40.
[22] L. Jørgensen, C. Vermehren, S. Bjerregaard, S. Froekjaer, Secondary structure alterations in insulin and growth hormone water-in-oil emulsions, Int. J. Pharm. 254 (2003) 7–10.
[23] L. Nielsen, R. Khurana, A. Coats, S. Frokjaer, J. Brange, S. Vyas, V.N. Uversky, A.L. Fink, Effect of environmental factors on the kinetics of insulin fibril formation: elucidation of the molecular mechanism, Biochemistry 40 (2001) 6036–6046.
[24] Y. Pocker, S.B. Biswas, Conformational dynamics of insulin in solution. Circular dichroic studies, Biochemistry 19 (1980) 4043–5049.
[25] J. Brange, L. Andersen, E.D. Laursen, G. Meyn, E. Rasmussen, Toward understanding insulin fibrillation, J. Pharm. Sci. 86 (1997) 517–525.